Archives of Razi Institute Journal
"Arch. Razi Inst."

Journal Homepage: https://archrazi.areeo.ac.ir/

Original Article

Antibacterial Photodynamic Therapy Using Zinc Phthalocyanine Against Multidrug-resistant *Pseudomonas aeruginosa* in Burn Infections

Forouhe Kiyani[1], Fereshte Ghandehari[1*], Mahnoosh Fatemi[2], Malahat Rezaee[3], Ali-Mohammad Ahadi[4]

1. Department of Microbiology, Fal.C., Islamic Azad University, Falavarjan, Iran.
2. Department of Biology, Fal.C., Islamic Azad University, Falavarjan, Iran.
3. Department of Biochemistry, Fal.C., Islamic Azad University, Falavarjan, Iran.
4. Department of Genetics, Faculty of Science, Shahrekord University, Shahrekord, Iran.

Use your device to scan and read the article online

How to cite this article Kiyani F, Ghandehari F, Fatemi M, Rezaee M, Ahadi A. Antibacterial Photodynamic Therapy Using Zinc Phthalocyanine Against Multidrug-resistant *Pseudomonas aeruginosa* in Burn Infections. Archives of Razi Institute Journal. 2025; 80(5):1247-1258. https://doi.org/10.32598/ARI.80.5.3485

https://doi.org/10.32598/ARI.80.5.3485

Article info:
Received: 25 Feb 2025
Accepted: 19 Mar 2025
Published: 01 Sep 2025

Keywords:
Antimicrobial photodynamic therapy (aPDT), Nanoemulsion, Photosensitizers, Zinc petalocyanine

ABSTRACT

Introduction: Due to the prevalence of MDR strains, alternative treatments such as antimicrobial photodynamic therapy (aPDT) have received much attention. This technique is an innovative technology that utilizes photosensitizers and generates active oxygen species. This study aimed to investigate the effectiveness of aPDT against multidrug-resistant (MDR) *Pseudomonas aeruginosa* using a nanoemulsion containing zinc phthalocyanine (NE/ZnPc) in a burn wound model under both in in vitro and in vivo conditions.

Materials & Methods: Optimization of PDT conditions —across different drug concentrations, different incubation times, different doses of laser radiation —was performed in vitro, and then the anti-biofilm effects of the optimal concentration against clinical isolates of MDR *P. aeruginosa* were investigated. Under in vivo conditions, male rats were divided into seven groups: Control, burn wound group, bacterial-infected burn wound, infected burn wound with laser treatment, infected wound treated with laser and drug (optimal concentration), infected wound treated with drug alone, and infected wound treated with nanoemulsion alone. The area of the burn wound was measured at the beginning and end of the experiment. Pieces of skin tissue were collected to perform histological studies and measure the expression of *EGFR* and *SOD1* genes.

Results: Based on the results, the drug at a concentration of 40 µg/mL encapsulated in nanoemulsion, a laser dose of 13 J/cm^2, and the incubation time of 2 hours were selected as optimal conditions. Under these conditions, 80% biofilm inhibition was observed. According to the histological results, NE/ZnPc-mediated aPDT and laser radiation reduced the burn

*** Corresponding Author:**
Fereshte Ghandehari, Assistant Professor.
Address: *Department of Microbiology, Fal.C., Islamic Azad University, Falavarjan, Iran.*
Tel: *+98 (31) 37420140*
E-mail: *fe_gh_2010@yahoo.com*

wound area, significantly accelerated the wound healing process, increased *EGFR* gene expression, and decreased *SOD1* gene expression to normal levels.

Conclusion: The promising antibacterial and anti-biofilm activity of NE/ClZnlPc-mediated aPDT against MDR *P. aeruginosa*, along with the increased expression of *EGFR* and *SOD1* levels in infected rat wounds, indicate that this treatment may be served as an alternative approach to eradicate MDR bacteria.

1. Introduction

Burns are the fourth most common cause of trauma worldwide. In extensive and deep burns, the immune system is weakened, making patients susceptible to invasive bacterial infections, which can lead to serious complications such as sepsis and toxic shock syndrome. Studies on burn wounds for determining bacterial profiles and antibiotic susceptibility of isolates have shown that *Pseudomonas aeruginosa* is one of the most common isolates in burn wounds, and many of these isolates exhibit antimicrobial resistance. This bacterium, through the production of various virulence factors, plays a role in the establishment of invasive infections [1, 2]. In addition to antimicrobial resistance, *P. aeruginosa*'s ability to form biofilms is considered a protective mechanism against physical, chemical, and environmental stresses [3, 4]. In burn infections, the pathophysiology of burn trauma is altered, so the dose and choice of antibiotic for treatment vary from person to person. On the other hand, inappropriate antibiotic prescription can lead to increased antibiotic resistance and the growth of multidrug-resistant (MDR) bacteria [5]. Therefore, currently, one of the best alternative treatments to antibiotics for infections caused by this bacterium is photodynamic therapy (PDT). This technique offers a promising approach to killing antibiotic-resistant bacteria using multiple light sources and photosensitizing dyes to reduce the number of gram-positive and gram-negative bacteria. The mechanisms responsible for bacterial damage via PDT include DNA damage, cell membrane degradation, alteration of membrane proteins, potassium ion leakage, and overall cell structure disruption [6]. The basis of PDT involves inducing oxidative stress by exposing a photosensitizing drug to light. In this approach, active oxygen species and free radicals weaken the microorganism's antioxidant defenses, ultimately leading to their elimination [7]. Phthalocyanines are the most common and effective photosensitizers used in PDT due to their high absorption in the red light region. Because of their macrocyclic hydrophobic structure, phthalocyanines tend to aggregate in biological solutions. Thus, there is a need for systems that encapsulate these drugs to protect them from metabolic breakdown, pH changes, or temperature fluctuations [8, 9]. Nanoemulsions, due to their high stability, low toxicity, and gradual and sustained drug release potential, as well as their ability to deliver lipophilic compounds, are suitable systems for facilitating the transfer of drugs across the plasma membrane and for intracellular delivery of lipophilic drugs [10]. The aim of the present study was to evaluate the inhibitory effects of PDT using zinc phthalocyanine in a nanoemulsion system against a clinical isolate of MDR *P. aeruginosa* obtained from burn infections under in vitro and in vivo conditions.

2. Materials and Methods

2.1. Isolation and identification of *P. aeruginosa* strains from burn infections

In this study, 30 *P. aeruginosa* isolates were collected from burn wounds of patients hospitalized at Taleghani Burn Hospital in Ahvaz. The isolates were identified using biochemical tests. The confirmed isolates were stored in LB broth (Merck, Darmstadt, Germany) medium containing 20% glycerol at -80 ˚C.

2.2. In vitro studies

2.2.1. Determination of antibiotic resistance patterns

According to the M100 protocol of the Clinical Laboratory Standards Institute (CLSI 2022) [11], 10 different antibiotics, including ceftazidime (30 µg), cefepime (30 µg), aztreonam (30 µg), imipenem (10 µg), meropenem (10 µg), amikacin (30 µg), ciprofloxacin (5 µg), piperacillin-tazobactam (100/10 µg), and gentamicin (10 µg), were selected (Padtan Teb Company).

Antibiotic resistance patterns of the strains were determined using the Kirby-Bauer disk diffusion method on Mueller-Hinton agar (Merck, Darmstadt, Germany) with a standard turbidity of 0.5 McFarland. The standard *P. aeruginosa* strain ATCC 27853 was used for quality control.

2.2.2. Nanoemulsion preparation

For preparation of a nanoemulsion containing zinc phthalocyanine (Sigma-Aldrich, Germany), hazelnut oil (Oseweh Company [Isfahan, Iran]) was used as the oil phase. Lipoid S75 (Lipoid, Germany) and PEG 40 (Kimyagaran Emrooz Chemical Industries Co., Iran) were used as surfactants. The spontaneous emulsification method was used for nanoemulsion preparation. In our previous study (results not shown), different ratios of oil and surfactants were examined to obtain the most stable nanoemulsion. The most appropriate values of ingredients were Lipoid S75:PEG (1:1), and an O/S ratio of 0.75. The O/S ratio was fixed for the preparation of nanoemulsions with different concentrations of ZnPc. At first, ZnPc was dissolved in ethanol at a concentration of 13.8 mM as a stock solution. Then, different volumes of the ZnPc solution were added to the oil-surfactants mixture to achieve a ZnPc concentration range of 10-80 µg/mL. Ethanol was then removed at 100 ˚C. In the final step, water was added dropwise and homogenized under simple stirring to obtain an equilibrium state. A blank nanoemulsion was prepared through this same procedure without ZnPc.

2.2.3. Optimization of PDT conditions

Optimization of PDT conditions, including drug concentrations, incubation times, and laser doses, was performed using a one-factor-at-a-time optimization method over three steps. In each step, optimization of a factor across various value ranges was carried out while the other two factors were kept constant at a certain value. Subsequently, 300 microliters of NE/ZnlPc at drug concentrations of 0, 10, 20, 40, 80 µg/mL were added to wells containing bacteria (optical ensity [OD] 600=0.55-0.06) and incubated for 30 minutes in the dark at 37 ˚C. Following the incubation period, the wells were exposed to a laser with a dose of 13 J/cm². To select the optimal incubation time, bacterial plates with the optimized drug concentration, as determined from the previous step, were incubated in the dark for 30 minutes, 1 hour, 2 hours, and 4 hours. In the next step, the bacterial plates with the optimized drug concentration and optimal incubation time were exposed to laser doses of 6, 13, and 20 J/cm². Each experiment was repeated three times. The decimal logarithm of CFU/mL was counted and normalized with respect to the CFU/mL of control cells (untreated).

2.2.4. Biofilm inhibition assay

100 µL of suspension of *P. aeruginosa* was added into 96-well titre plates. The conditions tested were: 1) control, which contained bacteria (B); 2) Bacteria exposed to optimal laser dose (B, L+); 3) Bacteria treated with optimal drug concentration without laser (B, d+, l-), 4) bacteria treated with optimal drug concentration with laser (B, d+, l+); 5) Bacteria under nanoemulsion treatment without laser (B, N+, L-); and 6) bacteria under nanoemulsion treatment with laser (B, N+, L+). Plates were incubated at 37 ˚C. After the incubation, the liquid suspension was removed, and 100 µL of 1% w/v aqueous solution of crystal violet was added. Following staining at room temperature for 30 minutes, the dye was removed, and the wells were washed thoroughly. Then, 95% ethanol was added and incubated for 15 minutes [12]. The reaction mixture was read spectrophotometrically at 570 nm. Inhibitio- mediated reduction of biofilm formation was calculated by the Equation 1:

1. $$\%\text{Inhibition Biofilm} = \frac{\text{OD in Control} - \text{OD in Treatment} \times 100}{\text{OD in control}}$$

2.3. In vivo studies

2.3.1. Animal grouping

Forty-two male rats (250±15 g) were obtained and kept at 20±2 ˚C, with a humidity of 50±5%, under a 12–12 hour's light/dark cycle, with access to food and water ad libitum. The rats were divided into seven groups as follows: Control group (no wound), burn wound group, burn-infected group with MDR *P. aeruginosa*, infected wound group treated with laser, infected wound group treated with laser and NE/ZnlPc (at optimal drug concentration), infected wound group treated with NE/ZnlP without laser, and infected wound group treated with nanoemulsion only.

2.3.2. Burn infection modeling in experimental groups

After shaving the back area and anesthetizing the rats using ketamine at a concentration of 100 mg/kg, a second-degree burn was induced on the back using a hot metal rod (100±2 ˚C) with a diameter of 2×2 cm [13]. Histopathological changes, including burn depth, were assessed by hematoxylin and eosin (H&E) staining and confirmed by a pathologist in a pilot study. The initial wound diameter was measured using calipers. Subse-

Table 1. Sequence of primers used in real-time PCR

Gene	Sequence (5′-3′)	Size (bp)	NCBI Accession Number
SOD1	F′-GAAGAGAGGCATGTTGGAGAC R: ACCACTGTACGGCCAATGATG	125	NM_011434.24
β-actin (control)	F: - GGACTCCTATGTGGGTGACG R: - AGGTGTGGTGCCAGATCTTC	119	NM_007393.5
EGFR	F: -GAGAACTGCCAGAAATTGACC R: GTACACCCCGCAGCACATTG	110	NM_207655.2

quently, the wounds were infected with 300 µL of a microbial suspension at a concentration of 1.5×10^8 CFU/mL, and the rats were then transferred to completely sterile cages.

2.3.3. PDT for burn wounds

After confirming infection in the wounds, the groups were treated with the optimized conditions of PDT as described above for seven consecutive days. At the end of the treatment period, the wound area was measured using vernier calipers. The results were compared between the groups at the end of the test.

2.3.4. Histopathological studies

A portion of the skin tissue from the control group and the burn sites of other groups was isolated and underwent dehydration, clearing, embedding, sectioning using a microtome, and staining with hematoxylin and eosin. Finally, the slides were examined under a light microscope.

2.3.5. Gene expression analysis using real-time polymerase chain reaction (PCR)

RNA extraction was performed using Trizol solution according to the company manual, and its concentration was measured by spectrophotometry, while integrity was assessed via gel electrophoresis. cDNA synthesis was conducted using the Sinaclon kit (RT5201) according to the specified protocol. Relative realtime RT-PCR was optimized based on $2^{-\Delta\Delta Ct}$ method [14, 15]. Samples were gently mixed without vortexing and placed in the real-time PCR device. The first stage included one cycle at 95 ˚C. for 5 seconds, the second stage involved one cycle at 95 ˚C for 10 minutes, and the third stage comprised 40 cycles at 60 ˚C for 30 seconds for denaturation, primer annealing, and extension. Primer sequences are listed in Table 1.

2.4. Statistical analysis

All data were expressed as Mean±SD and analyzed using one-way analysis of variance (ANOVA) with SPSS software, version 22, with a significance level of $P\leq0.05$. To statistically analyze relative gene expression changes among different treatment groups compared to controls, GraphPad Prism software, version 7 was used.

3. Results

3.1. In vitro studies

Selection of MDR strain and optimization of PDT among the 30 clinical isolates of *P. aeruginosa*, strain P18 demonstrated resistance to five different antibiotics from various classes. This MDR isolate was selected for further experiments. Based on the optimization results (Figure 1), the optimal conditions for PDT were determined as follows: A drug concentration of 40 µg/mL, a laser dose of 13 J/cm², and an incubation time of two hours.

3.2. Anti-biofilm effects of PDT

The results of the anti-biofilm effects of zinc phthalocyanine (Figure 2) demonstrated that the combination of laser and NE/ZnlPc exhibited a significant increase in anti-biofilm activity compared to laser alone or blank nanoemulsion. This increase was notably more pronounced in the group treated with NE/ZnlPc under laser ($P\leq0.001$). However, in the groups treated with nanoemulsion and NE/ZnlPc without laser, there was no significant difference in biofilm inhibition percentage compared to the control group.

3.3. In vivo study results

3.3.1. Comparison of burn wound diameter among experimental groups

According to Figure 3, a reduction in wound diameter was observed only in the group of rats treated with NE/ZnlPc under laser compared to the burn wound group

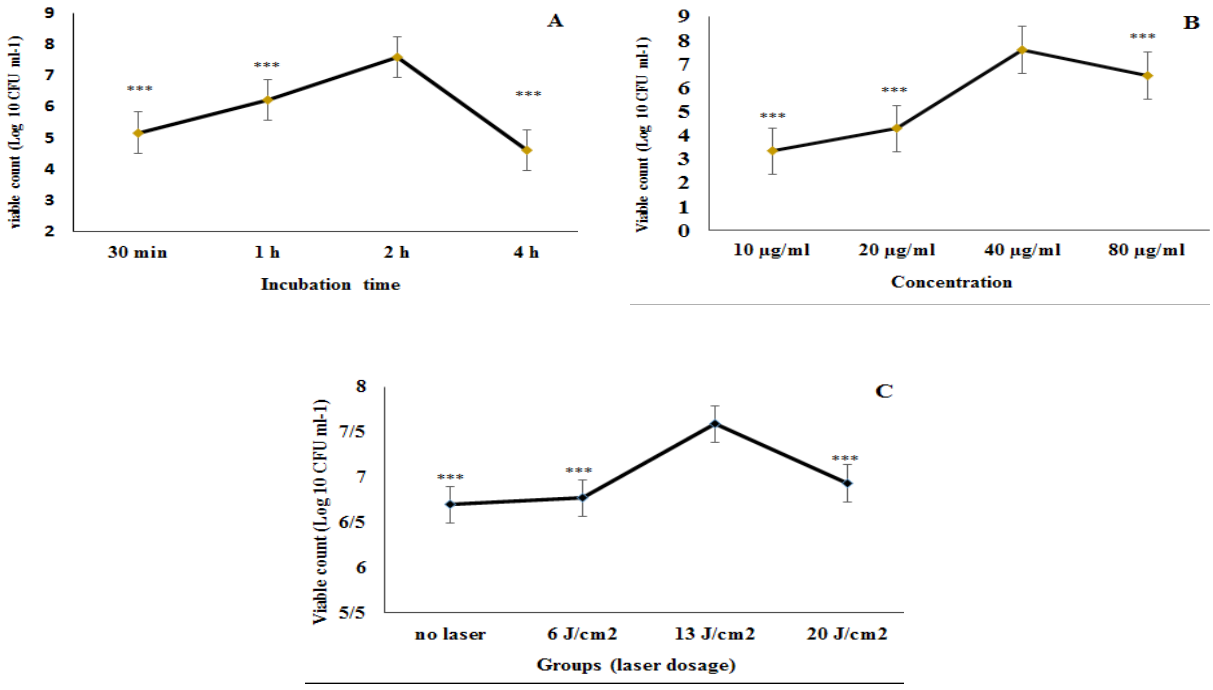

Figure 1. Photodynamic therapy optimization

A) Comparison of the effect of mean incubation times with a drug concentration of 40 µg/mL and a laser dose of 13 J/cm² on the viable count (Log 10 CFU/mL); B) Comparison of different drug concentrations with a two-hour incubation time and a laser dose of 13 J/cm²; C) Comparison of various laser doses with a drug concentration of 40 µg/mL and a two-hour incubation time. significant difference

***P≤0.001.

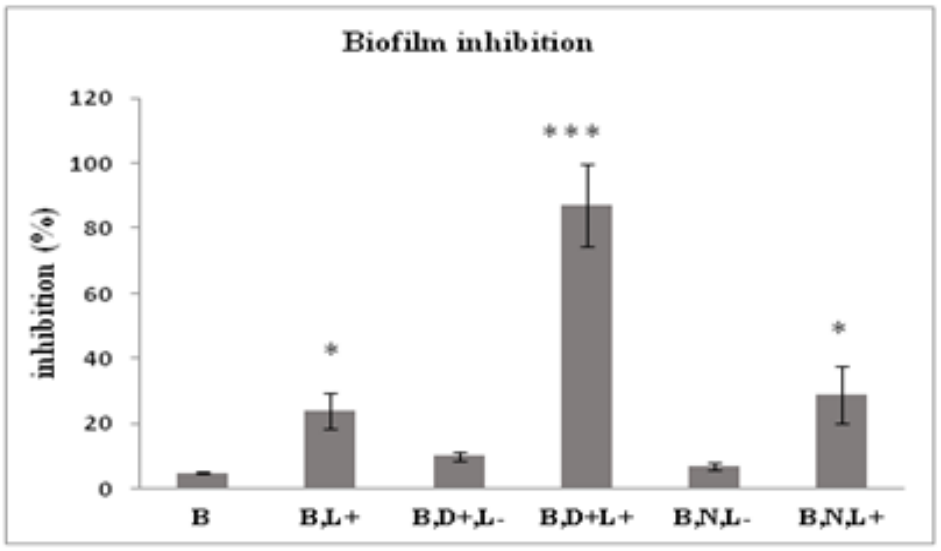

Figure 2. Comparison of biofilm inhibition percentage between experimental groups

Note: Data are expressed as Mean±SD. Significance levels include ***P≤0.001, **P≤0.01, *P≤0.05. B) Control group containing bacteria; B, L+) Bacteria exposed to optimal laser dose; B, D+, L-) Bacteria treated with optimal drug concentration without laser; B, D+, L+) Bacteria treated with optimal drug concentration with laser; B, N+, L-) Bacteria treated with nanoemulsion without laser; (B, N+, L+) Bacteria treate with nanoemulsion with laser.

Archives of Razi Institute Journal

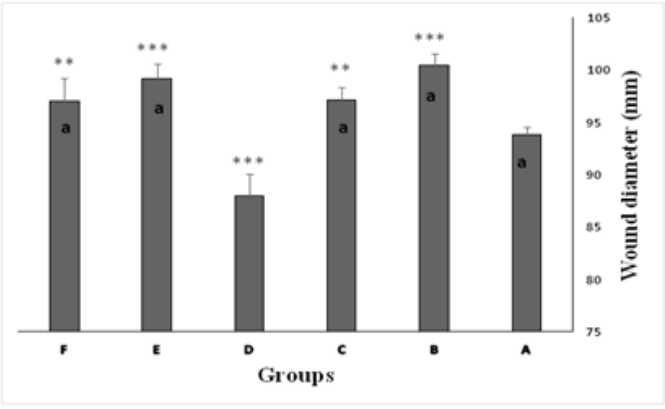

Figure 3. Burn wound diameter of experimental groups at the end of the test period

Note: Data are expressed as Mean±SD. a indicates P≤0.001 compared to experimental groups treated with the NE/ZNlPc under laser exposure. Stars represent comparisons of other groups with the burn-only group. ***P≤0.001, **P≤0.01, *P≤0.05.

(P≤0.001). These findings indicated that the wound diameter in this group was significantly smaller compared to all other groups (P≤0.001).

3.3.2. Histopathological examination

In the control group (Figures 4A1 and 4A2), all major layers of the skin —including the epidermis, dermis, and hypodermis —were clearly identifiable, along with normal hair follicles, blood vessels, and sebaceous glands. In the burn wound group (B1), the epidermis was completely absent, and collagen fibers in the dermis appeared homogeneously aligned. At higher magnification (B2), numerous blisters were observed in the dermis. In groups with infected burn wounds (C1), there was a complete loss of the epidermis, bacterial colonies on the surface layer, and extensive dermal damage (C2), along with inflammatory cell infiltration from the subcutaneous to the muscle layers (C3).

In the group with infected wounds treated only with the drug (D1), the epidermis was still absent, with extensive dermal damage, hyperemia, bacterial colonies, and homogeneously arranged collagen fibers (D2). Similarly, in the group treated with nanoemulsion alone (E1), the epidermis did not form, while hyperemia, homogeneously arranged collagen fibers, and extensive inflam-

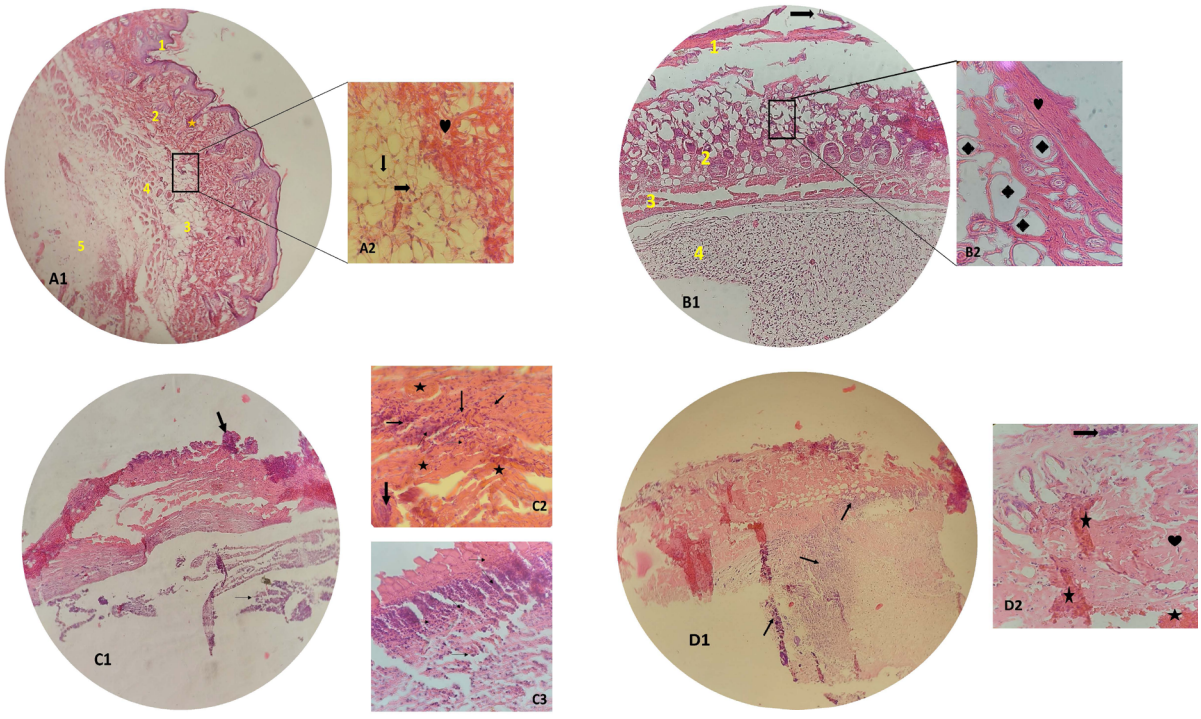

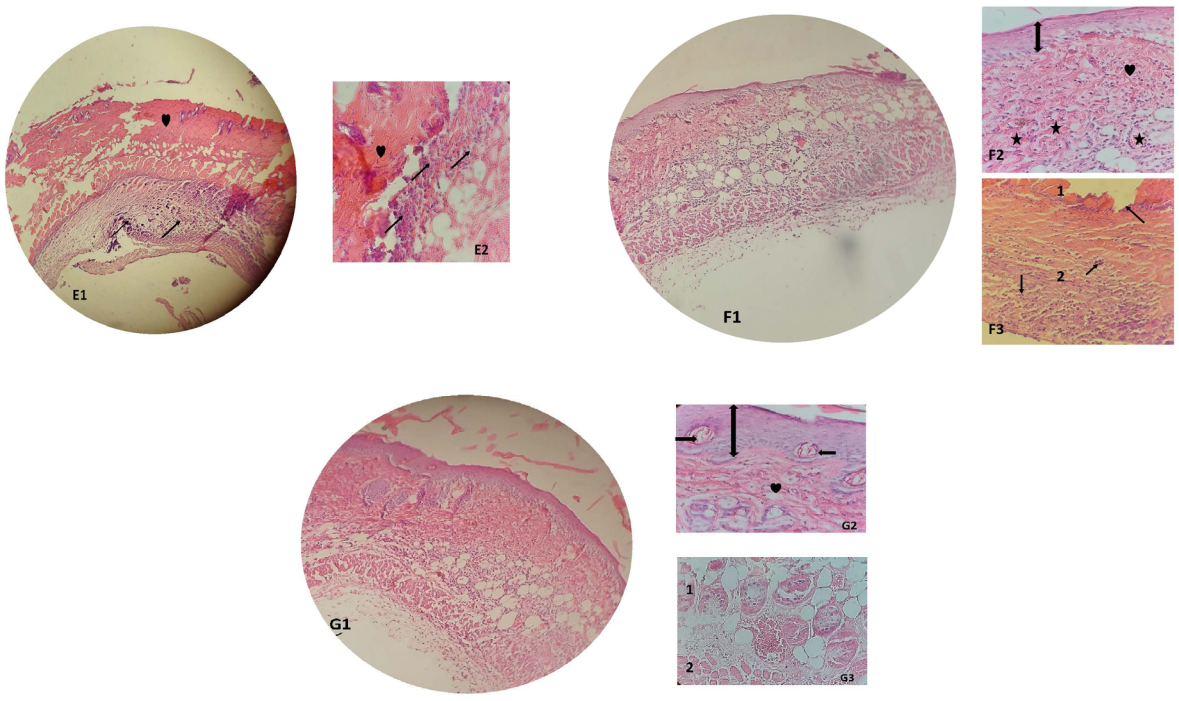

Figure 4. Histological sections of skin tissue in control and experimental groups

Skin of the control group: A1) Section of control group skin tissue showing layers 1 to 5 —epidermis, dermis, hypodermal adipose tissue, muscle tissue, and subcutaneous layer —with a completely normal structure at 40× magnification. The star symbol indicates a hair follicle. A2) Higher magnification (100×) image of normal skin tissue in the control group, illustrating normal collagen fibers (indicated by the arrow) and normal adipose tissue (indicated by the heart shape). B1) Section of skin tissue from rats with induced burns. Layer 1 shows the dermis, with visible destruction and separation from underlying layers 2 to 4 (hypodermis, muscle tissue, and subcutaneous layer). B2) Collagen fibers in a homogeneous arrangement (indicated by the heart) and fluid-filled blisters (indicated by the star) are visible in the dermal region at 100× magnification. C1) Skin tissue from the burn infection group, showing complete absence of the epidermis, with bacterial colonies on the surface layer (indicated by the arrow) and extensive dermal damage at 40× magnification. C2 and C3) Sections from the burn infection group at 100× magnification. In C2, a thick arrow indicates bacterial colonies, a thin arrow marks invasive inflammatory cells in the dermis, and stars denote blood vessels. In C3, arrows illustrate the invasion of inflammatory cells from the subcutaneous layer toward the muscle layer.

Skin of the burn infection treated with the drug: D1: Similar to the previous group, the epidermis is not observed, and the dermis appears highly disordered with extensive damage. Arrows indicate inflammatory cells. D2: Shows a bacterial colony (arrow), hyperemia (star), and homogenously arranged collagen fibers. E1: The epidermis is still not visible, similar to the previous group. Inflammatory cells are widely present in the subcutaneous layer (arrow). The heart symbol indicates homogenously arranged collagen fibers. E2: At higher magnification, the presence of inflammatory cells in the hypodermis and deeper dermal areas is evident. Bacterial colony and hyperemia in tissue slides from this group were less prominent than in previous groups.

Skin of the burn-infected group treated with laser: F1: The epidermal layer is visible, and other layers appear almost normal. F2: The double-headed arrow indicates a thin epidermis; hair follicles and dermal papillae are still absent. Stars represent hyperemia, and the heart symbol indicates collagen fibers with a relatively normal arrangement. F3: Arrows indicate the presence of inflammatory cells in the subcutaneous (2) and muscle (1) layers.

Skin of the burn-infected group treated with NE/ZnlPc and laser: G1: This figure shows an epidermis with thickness close to the control group, along with the presence of hair follicles and dermal papillae; other layers appear normal. G2: The double-headed arrow shows the thickness of the epidermis. Arrows indicate cross-sections of hair follicles, and the heart symbol represents the normal arrangement of collagen. G3: Numbers 1 and 2 represent the hypodermis and muscle layer, respectively, with a very low number of inflammatory cells in these areas.

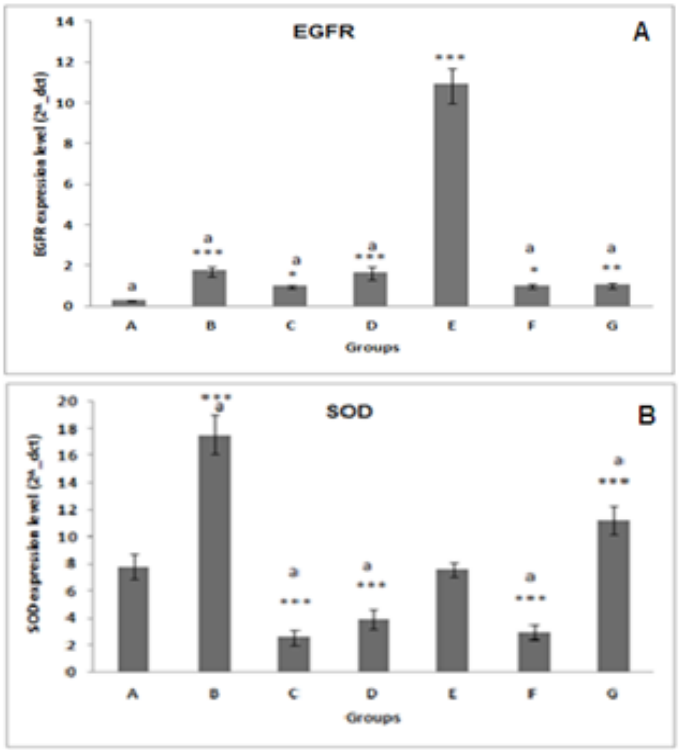

Figure 5. Analysis of *EGFR* (A) and *SOD1* (B) gene expression changes in groups

Note: Data are presented as Mean±SD. Stars indicate comparisons between the control group and other groups, while "a" denotes comparisons of group E with other groups at the P≤0.001 level. Significance levels are as follows: ***P≤0.001, **P≤0.01, *P≤0.05. Groups A to G are as follows: Control group, burn group, burn infection group, laser-treated group, NE/ZnlPc treated under laser, drug-treated group, and nanoemulsion-treated group.

matory cell infiltration in the hypodermis and underlying dermal layers were observed (E2). In the infected burn wound group treated with laser exposure, a thin epidermal layer was present, though hair follicles and dermal papillae were still absent (F1). At higher magnification, collagen fibers exhibited a relatively normal arrangement, but inflammatory cells were still observed in the subcutaneous and muscle layers (F2, F3). Significant improvement was observed following burn treatment with both the drug and the nanoemulsion (G1). The epidermal thickness was similar to that of the control group, with the presence of hair follicles and dermal papillae. Other layers appeared normal, with visible, normally arranged hair follicles and collagen, and a decrease in inflammatory cells in the hypodermis (G2, G3).

3.3.3. EGFR and SOD1 gene expression changes in experimental groups

The results of the comparison of *EGFR* gene expression between experimental groups and the control group revealed a significant increase (Figure 5A). This increase was particularly prominent in groups B, D, and E —especially in group E (P≤0.001).

According to Figure 5B, *SOD1* expression increased in groups B and G, while significant decreases (P≤0.001) were observed in groups C, D, and F. Upon comparing the group treated with NE/ZnlPc under laser with other groups, no significant difference in the expression level of this gene was observed compared to the control group.

4. Discussion

Treatment of burn wound infections is a major medical challenge. A high percentage of mortality in burn units is attributed to post-incident infections, with *P. aeruginosa* being the most prevalent colonizing pathogen in burn wounds. The main issue in treating these infections is the formation of resilient biofilms that are resistant to most available treatments. Antibiotic treatment can have side effects, posing a threat to burn patients' health. For deep burn wounds, antibiotic use may inhibit skin tissue regeneration and treatment of edema. Thus, the development of new antibacterial therapies, especially for burn infections caused by MDR bacteria, is crucial. Increasing microbial resistance to antimicrobial compounds necessitates the exploration of new therapeutic approaches to treat bacterial infections.

One promising approach is antimicrobial PDT (aPDT), which is effective against MDR bacteria [16]. The technique relies on inducing oxidative stress by exposing a photosensitizing drug to laser radiation. Optimization of this method was performed using NE/ZnlPc at different concentrations, various laser doses, and incubation times on *P. aeruginosa* isolates from patients with burn wounds and MDR strains. The results showed that the highest inhibitory effect was achieved with 40 µg/mL of the drug, two-hour incubation time, and 13 J/cm² laser dose. Additionally, the anti-biofilm effect of the optimized conditions was examined on the target isolate. The findings indicated that while laser treatment and nanoemulsion alone increased biofilm inhibition, the highest inhibition percentage was observed in the group treated with both the drug and laser. The results of antibacterial photodynamic studies by Anju et al. [17] using carbon nanotubes conjugated with malachite green dye and irradiated for three minutes with a red laser at a wavelength of 660 nm, showed growth and biofilm inhibition in *P. aeruginosa* and *Staphylococcus aureus* strains. Ribeiro and colleagues, using PDT with curcumin extract on methicillin-resistant *S. aureus* biofilm, observed a significant reduction in biofilm inhibition. Scanning electron microscope (SEM) micrograph evaluations also demonstrated a reduction in bacterial cells and extracellular polymeric matrix after PDT. It appears that the zinc phthalocyanine nanoemulsion, due to its small size, can penetrate bacterial cells even within biofilm clusters, potentially disrupting metabolic activity and inhibiting bacterial cell growth [18]. In continuation of this research, the optimal drug concentration, incubation time, and laser dose were evaluated in vivo on burn infections in rat models. The results of wound diameter comparisons among the experimental groups after the treatment period revealed a significant reduction in wound size in the group of rats treated with the drug-containing nanoemulsion under laser irradiation compared to other groups, aligning with histopathological studies. Histopathological analysis is considered the gold standard for assessing wound healing progress and determining epidermal epithelialization. The skin is the most critical barrier for human resistance against external threats. Wound healing after skin injuries, such as burns, involves a complex series of processes, including cell proliferation and migration, cytokine secretion, and inflammatory responses [19]. Inflammation represents the initial stage of wound healing and occurs nearly concurrently with hemostasis. As the inflammatory response progresses, various cytokines and growth factors activate and induce the proliferation, migration, and differentiation of repair cells, leading to biological behaviors such as epithelialization, angiogenesis, and collagen deposition. Continuous tissue remodeling, with fibroblasts differentiating into myofibroblasts, contributes to wound contraction and the restoration of skin integrity [20]. Bacterial infections can prolong the inflammatory phase, disrupt epithelial layer formation and collagen deposition, and ultimately impair wound healing [21]. Previous studies have demonstrated the positive impact of PDT on tissue healing and repair in infected wounds [22, 23]. In the present study, the control group's tissue structure appeared completely normal, with appropriately thick dermis, epidermis, and hypodermis layers, including hair follicles, sebaceous glands, and blood vessels. In the burn wound group, epidermal destruction, numerous blisters, and collagen fiber disarray were evident in the affected area. In the group with burn wounds infected by *P. aeruginosa*, there was more severe destruction of the epidermal and dermal layers, with numerous *P. aeruginosa* colonies and inflammatory cell invasion. In this study, zinc phthalocyanine's penetration was enhanced by the nanoemulsion system, likely resulting in deeper infection clearance from tissue surfaces and faster healing. Results from Figueiredo-Godoi and colleagues on PDT using methylene blue sensitizer on *Acinetobacter baumannii*-infected burns also indicated this sensitizer's potential to penetrate the cell wall of gram-negative bacteria, ultimately inhibiting and bacterial growth improving wound healing [24]. In the present study, following burn induction, the *SOD1* expression level significantly increased. However, after inducing infection in the wound, the expression level of this gene decreased. In the two infected groups treated with laser alone or drug alone, the enzyme level also decreased. Consistent with this study, antioxidant enzyme activity was also found to decrease in diabetic rats with infected wounds compared to the control group [7]. Superoxide dismutase (SOD) is the most important and primary antioxidant enzyme in all aerobic organisms, playing a key role in directly reducing reactive oxygen metabolites and serving as the first line of defense against superoxide radicals (O_2), converting superoxide anions to H_2O_2 and repairing cells. Previous research has shown that SOD1 levels increase during wound healing and accelerate the healing process [25, 26]. Therefore, it appears that the reduction in enzyme expression following infection is due to increased oxidative stress caused by the overproduction of free radicals, which leads to the oxidation and subsequent denaturation of the enzyme. It seems that laser or drug alone did not have a significant effect on reducing oxidative stress. PDT increases oxidative stress in bacteria, leading to their elimination; this process prevents the immune system cells from engaging the bacteria in a violent fight. In this study, PDT us-

ing NE/ZnlPc under laser irradiation brought the SOD1 enzyme expression level closer to normal. During wound healing, various inflammatory cells such as neutrophils, macrophages, endothelial cells, and fibroblasts produce reactive oxygen species, which can increase the levels of these radicals and cause significant cell damage. Enhancing the body's antioxidant system can help reduce these radicals and facilitate the healing process [27]. In the study by Kalay et al. wounds induced in rats were treated with epidermal growth factor (EGF) therapy. The levels of thiobarbituric acid reactive substances (TBARS) decreased, while ascorbic acid, glutathione, and SOD activity levels increased —especially on the fifth day after treatment —gradually returning to normal by day 15. These researchers suggested that EGF may act like an antioxidant, consuming toxic oxidative compounds, enhancing endogenous antioxidants, and ultimately promoting wound healing [28]. Given the possible link between growth factors and antioxidants, the expression level of *EGFR* was also evaluated in skin tissue in this study. EGFR is a glycoprotein with tyrosine kinase activity and plays a vital role in regulating cellular signaling pathways. This tyrosine kinase receptor (RTK) belongs to the larger family of ErbB proto-oncogenes and is involved in cell survival, proliferation, angiogenesis, and invasion. EGF plays an important role in wound healing across various tissues, including the skin, cornea, oral mucosa, and stomach [29, 30]. Numerous studies have highlighted the positive effects of growth factors on enhancing and restoring EGFR in the healing of skin wounds in animals [29, 31]. EGFR stimulates fibroblasts to synthesize vascular endothelial growth factor (VEGF) and other growth factors involved in angiogenesis, which promotes wound healing by re-epithelialization, stimulation of angiogenesis, collagen deposition, mypfibroblast differentiation, and extracellular matrix remodeling [31, 32]. In the present study, *EGFR* expression levels increased in all experimental groups compared to the control group, with the highest increase observed in burn-infected rats treated with the drug-containing nanoemulsion exposed to laser. This suggests the potential impact of this therapeutic method on wound healing, and the histopathological results were consistent with these findings. The increased expression of *EGFR* and *SOD1* in infected rat wounds following PDT with NE/ZnlPc under laser irradiation (under optimal conditions) demonstrates the positive impact of this therapeutic method in the present study. Given the observed re-epithelialization, along with neovascularization and reduced inflammation in tissue samples, this approach may serve as an alternative to antibiotic treatments for burn infections.

Ethical Considerations

Compliance with ethical guidelines

All procedures were carried out according to the guidelines for working with laboratory animals, approved by the Ethics Committee of Falavarjan Branch, Islamic Azad University, Falavarjan, Iran (Code: IR.IAU.FALA.REC.1399.012).

Data availability

The data that support the findings of this study are available upon request from the corresponding author.

Funding

This research has not received any funding from funding organizations in the government, commercial, or non-profit sectors.

Authors' contributions

Conceptualization, study design, data acquisition, and writing the original draft: Fereshte Ghandehari, Forouhe Kiyani and Mahnoosh Fatemi; Data analysis and interpretation: Malahat Rezaee, Fereshte Ghandehari and Mahnoosh Fatemi; Statistical analysis: Mahnoosh Fatemi and Malahat Rezaee; Review and editing: Fereshte Ghandehari, Forouhe Kiyani, Ali-Mohammad Ahadi and Mahnoosh Fatemi.

Conflict of interest

The authors declared no conflict of interest.

Acknowledgements

The authors are grateful to the Faculty of Basic Sciences, Falavarjan Branch, Islamic Azad University, Falavarjan, Iran, for their cooperation and the supply of experimental equipment.

References

[1] Spernovasilis N, Psichogiou M, Poulakou G. Skin manifestations of Pseudomonas aeruginosa infections. Curr Opin Infect Dis. 2021; 34(2):72-9. [DOI:10.1097/QCO.0000000000000717] [PMID]

[2] Yang T, Tan Y, Zhang W, Yang W, Luo J, Chen L, et al. Effects of ALA-PDT on the healing of mouse skin wounds infected with pseudomonas aeruginosa and its related mechanisms. Front Cell Dev Biol. 2020; 8:585132. [DOI:10.3389/fcell.2020.585132] [PMID]

[3] D'Arpa P, Karna SLR, Chen T, Leung KP. Pseudomonas aeruginosa transcriptome adaptations from colonization to biofilm infection of skin wounds. Sci Rep. 2021; 11(1):20632. [DOI:10.1038/s41598-021-00073-4] [PMID]

[4] Kranjec C, Morales Angeles D, Torrissen Mårli M, Fernández L, García P, Kjos M, et al. Staphylococcal Biofilms: Challenges and Novel Therapeutic Perspectives. Antibiotics (Basel). 2021; 10(2):131.[DOI:10.3390/antibiotics10020131] [PMID]

[5] Tsolakidis S, Freytag DL, Dovern E, Alharbi Z, Kim BS, Houschyar KS, et al. Infections in burn patients: A retrospective view over seven years. Medicina. 2022; 58(8):1066 [DOI:10.3390/medicina58081066] [PMID]

[6] Badran Z, Rahman B, De Bonfils P, Nun P, Coeffard V, Verron E. Antibacterial nanophotosensitizers in photodynamic therapy: An update. Drug Discov Today. 2023; 28(4):103493. [DOI:10.1016/j.drudis.2023.103493] [PMID]

[7] Sedeh SS, Fatemi M, Ghandehari F. Antimicrobial Photodynamic Therapy Using Zinc Phthalocyanine Nanoemulsion Against Infected Wounds in Diabetic Rats. Avicenna J Clin Microbiol Infect .2023; 10(3):120-5. [DOI:10.34172/ajcmi.3496]

[8] Bunin DA, Martynov AG, Gvozdev DA, Gorbunova YG. Phthalocyanine aggregates in the photodynamic therapy: dogmas, controversies, and future prospects. Biophys Rev. 2023; 15(5):983-98. [DOI:10.1007/s12551-023-01129-7] [PMID]

[9] Ömeroğlu İ, Durmuş M. Water-soluble phthalocyanine photosensitizers for photodynamic therapy. Turk J Chem. 2023; 47(5):837-63. [DOI:10.55730/1300-0527.3583] [PMID]

[10] Felifel NT, Sliem MA, Kamel Z, Bojarska J, Seadawy MG, Amin RM, et al. Antimicrobial photodynamic therapy against escherichia coli and staphylococcus aureus using nanoemulsion-encapsulated zinc phthalocyanine. Microorganisms. 2023; 11(5):1143. [DOI:10.3390/microorganisms11051143] [PMID]

[11] Gaur P, Hada V, Rath RS, Mohanty A, Singh P, Rukadikar A. Interpretation of antimicrobial susceptibility testing using European Committee on Antimicrobial Susceptibility Testing (EUCAST) and Clinical and Laboratory Standards Institute (CLSI) breakpoints: Analysis of agreement. Cureus. 2023; 15(3):e36977. [Link]

[12] Namasivayam SKR, Roy EA. Anti biofilm effect of medicinal plant extracts against clinical isolate of biofilm of Escherichia coli. Int J Pharm Pharm Sci. 2013; 5(2):486-9. [Link]

[13] Pavliuk B, Stechyshyn IR, Kramar S, Chubka MA, Hroshovyi T. Therapeutic efficacy of the developed gel "Xeliogel" on a burn wound model in rats. Pol Med J, 2020; XLVII(287):331–4. [Link]

[14] Livak KJ, Schmittgen TD. Analysis of relative gene expression data using real-time quantitative PCR and the 2(-Delta Delta C(T)) Method. Methods. 2001; 25(4):402-8. [DOI:10.1006/meth.2001.1262] [PMID]

[15] Tanaka Y, Yamaguchi A, Fujikawa T, Sakuma K, Morita I, Ishii K. Expression of mRNA for specific fibroblast growth factors associates with that of the myogenic markers MyoD and proliferating cell nuclear antigen in regenerating and overloaded rat plantaris muscle. Acta Physiol (Oxf). 2008; 194(2):149-59. [DOI:10.1111/j.1748-1716.2008.01866.x] [PMID]

[16] Feng Y, Coradi Tonon C, Ashraf S, Hasan T. Photodynamic and antibiotic therapy in combination against bacterial infections: Efficacy, determinants, mechanisms, and future perspectives. Adv Drug Deliv Rev. 2021; 177:113941. [DOI:10.1016/j.addr.2021.113941] [PMID]

[17] Anju VT, Paramanantham P, Siddhardha B, Sruthil Lal SB, Sharan A, Alyousef AA, et al. Malachite green-conjugated multi-walled carbon nanotubes potentiate antimicrobial photodynamic inactivation of planktonic cells and biofilms of Pseudomonas aeruginosa and Staphylococcus aureus. Int J Nanomedicine. 2019; 14:3861-3874. [DOI:10.2147/IJN.S202734] [PMID]

[18] Ribeiro IP, Pinto JG, Souza BMN, Miñán AG, Ferreira-Strixino J. Antimicrobial photodynamic therapy with curcumin on methicillin-resistant Staphylococcus aureus biofilm. Photodiagnosis Photodyn Ther. 2022; 37:102729. [DOI:10.1016/j.pdpdt.2022.102729] [PMID]

[19] Shpichka A, Butnaru D, Bezrukov EA, Sukhanov RB, Atala A, Burdukovskii V, et al. Skin tissue regeneration for burn injury. Stem Cell Res Ther. 2019; 10(1):94. [DOI:10.1186/s13287-019-1203-3] [PMID]

[20] Shi Z, Yao C, Shui Y, Li S, Yan H. Research progress on the mechanism of angiogenesis in wound repair and regeneration. Front Physiol. 2023; 14:1284981. [DOI:10.3389/fphys.2023.1284981] [PMID]

[21] Lin Y, Chen Z, Liu Y, Wang J, Lv W, Peng R. Recent advances in nano-formulations for skin wound repair applications. Drug Des Devel Ther. 2022; 16:2707-28. [DOI:10.2147/DDDT.S375541] [PMID]

[22] Gu R, Fei S, Liu Z, Liu X, Fang X, Wu H, et al. Effects of photodynamic therapy in patients with infected skin ulcers: A meta-analysis. Int Wound J. 2024; 21(3):e14747. [DOI:10.1111/iwj.14747] [PMID]

[23] Tong A, Tong C, Fan J, Shen J, Yin C, Wu Z, et al. Prussian blue nano-enzyme-assisted photodynamic therapy effectively eradicates MRSA infection in diabetic mouse skin wounds. Biomater Sci. 2023; 11(18):6342-56. [DOI:10.1039/D3BM01039B] [PMID]

[24] Figueiredo-Godoi LMA, Garcia MT, Pinto JG, Ferreira-Strixino J, Faustino EG, Pedroso LLC, et a. Antimicrobial Photodynamic Therapy Mediated by Fotenticine and Methylene Blue on Planktonic Growth, Biofilms, and Burn Infections of Acinetobacter baumannii. Antibiotics (Basel). 2022; 11(5):619. [DOI:10.3390/antibiotics11050619] [PMID]

[25] Wink DA, Hines HB, Cheng RY, Switzer CH, Flores-Santana W, Vitek MP, et al. Nitric oxide and redox mechanisms in the immune response. J Leukoc Biol. 2011; 89(6):873-91. [DOI:10.1189/jlb.1010550] [PMID]

[26] Qiu X, Wu Y, Zhang D, Zhang H, Yu A, Li Z. Roles of oxidative stress and raftlin in wound healing under negative-pressure wound therapy. Clin Cosmet Investig Dermatol. 2021; 14:1745-53. [DOI:10.2147/CCID.S334248] [PMID]

[27] Salih Ağırtaş M, Karataş C, Özdemir S. Synthesis of some metallophthalocyanines with dimethyl 5-(phenoxy)-isophthalate substituents and evaluation of their antioxidant-antibacterial activities. Spectrochim Acta A Mol Biomol Spectrosc. 2015; 135:20-4. [DOI:10.1016/j.saa.2014.06.139] [PMID]

[28] Kalay Z, Cevher SC. Oxidant and antioxidant events during epidermal growth factor therapy to cutaneous wound healing in rats. Int Wound J. 2012; 9(4):362-71. [DOI:10.1111/j.1742-481X.2011.00895.x] [PMID]

[29] Alemdaroğlu C, Değim Z, Celebi N, Zor F, Oztürk S, Erdoğan D. An investigation on burn wound healing in rats with chitosan gel formulation containing epidermal growth factor. Burns. 2006; 32(3):319-27. [DOI:10.1016/j.burns.2005.10.015] [PMID]

[30] Güleç Peker EG, Coşkun Ş, Ebegil M, Acartürk F. Effect of exogenous epidermal growth factor (EGF) on nonenzymatic antioxidant capacities and MPO activity of wound tissue. Med Chem Res. 2010; 19:533-40. [DOI:10.1007/s00044-009-9210-z]

[31] Shanmugapriya K, Kim H, Kang HW. EGFR-conjugated hydrogel accelerates wound healing on ulcer-induced burn wounds by targeting collagen and inflammatory cells using photoimmunomodulatory inhibition. Mater Sci Eng C Mater Biol Appl. 2021; 118:111541. [DOI:10.1016/j.msec.2020.111541] [PMID]

[32] Mao Y, Ma J, Xia Y, Xie X. The overexpression of Epidermal Growth Factor (EGF) in HaCaT cells promotes the proliferation, migration, invasion and transdifferentiation to epidermal stem cell immunophenotyping of Adipose-Derived Stem Cells (ADSCs). Int J Stem Cells. 2020; 13(1):93-103. [DOI:10.15283/ijsc18146] [PMID]